STScI | SPACE TELESCOPE SCIENCE INSTITUTE

**Instrument Science Report COS 2018-15(v1)**

# Performance of the CalCOS FUV WAVECORR Algorithm at Lifetime Position 4

James White[1], Nick Indriolo[1], and Julia Roman-Duval[1]

[1] Space Telescope Science Institute, Baltimore, MD

4 February 2019

**ABSTRACT**

*In this ISR we report on the results of our investigation into the impact on the CalCOS pipeline module WAVECORR of moving COS FUV operations to lifetime position four (LP4). The WAVECORR module determines the location of the wavelength calibration (wavecal) spectrum on the detector relative to a template and then uses this shift to determine the zero-point of the wavelength scale. The wavecal spectrum at LP4 falls at the LP2 location, which suffers from gain sag and, in turn, heavily distorts the profile of the wavecal spectrum. To test the performance of WAVECORR under LP4 conditions, we created simulations that showed that under these conditions, WAVECORR could fail to find the shift between the wavecal spectrum and template, with the settings G160M/1611 and G160M/1623 failing most often. Program 14869, "COS/FUV Wavecorr at LP4" (PI D. Sahnow) was created to validate the results of the simulations by obtaining on-orbit data. Using those data, we tested the simulation results for G160M/1611 and G160M/1623 and characterized the effect of gain sag on WAVECORR measurements of the shift between the wavecal spectrum and the lamp template. The simulations were validated and showed that, when WAVECORR did not fail outright, the error produced in calibration was not typically increased. We show that by changing a constant parameter that is used by CalCOS as a threshold for rejecting bad matches when performing the cross-correlation between the wavecal spectrum and lamp template, we can obtain reliable WAVECORR results for data at LP4.*

## Contents



## 1. Introduction

The Cosmic Origins Spectrograph's (COS's) far ultraviolet (FUV) detector degrades with use, which results in a decreased ability of the detector to convert incoming photons into electron clouds, an effect referred to as gain sag.

In a gain-sagged region, the strength of the charge cloud per event, or pulse height, generated by the individual photons that strike the detector is greatly reduced. This can result in events being flagged and discarded by the COS calibration pipeline (CalCOS) and can lead to "holes" (gain-sag holes) on areas of the detector that are exposed to large flux levels such as from Lyman $\alpha$ airglow or flux from routinely observed targets. At lower pulse heights, the locations of events are also more susceptible to being misidentified (walk), which can affect the resolution. Sahnow et al. (2011, ISR 2011-05) and Sahnow (2018, TIR 2018-03) provide detailed discussions of gain sag and walk.

To mitigate the effects of gain sag, lifetime positions (LPs) were established. LPs define the position on the detector where science spectra will fall in the cross-dispersion (XD) direction after passing through the Primary Science Aperture (PSA) or Bright Object Aperture (BOA). This investigation and analysis was conducted for the fourth LP, LP4, located $\approx 5''$ (or $\approx 54$ pixels) below the first LP, LP1, in the XD direction.

The Wavelength Calibration Aperture (WCA), which is located $\approx 9''$ ($\approx 98$ pixels) above the PSA in the XD direction, is used in the wavelength calibration process. Light from one of two internal Pt-Ne wavelength calibration lamps passes through the WCA to produce a lamp, or wavecal, spectrum. Wavecal spectra are typically taken concurrently with science data in TAGFLASH mode, which is determined with rules described by Keyes (2011, ISR 2011-04). In the WAVECORR step of CalCOS, the wavecal spectra are compared to a template to measure and remove shifts in the science spectrum due to small motions (drift) of the Optics Select Mechanism (OSM) during the exposure and

uncertainty between the commanded position of the OSM and the real location (OSM uncertainty). At LP4, the WCA places the wavecal spectra on top of LP2, which is severely gain sagged after 2.5 years of operations at that LP. Because of this, the lamp spectra taken at LP4 will be strongly affected by gain sag as lines fall in and out of the worst-affected regions causing substantial loss in counts in the spectra. We use two methods in this investigation to test the effects of gain sag on wavecal spectra. First, we simulate LP4 data by modifying existing LP3 WCA data. Next, we analyze data taken at LP4 in program 14869, "COS/FUV Wavecorr at LP4" (PI D. Sahnow), created specifically for this purpose.

## 2. Testing WAVECORR at LP4 with Simulated Spectra

### *2.1 Calculating New PHA Values Based on Differences in Gain*

In order to test the effects of gain sag on the WAVECORR step of CalCOS, we created simulated LP4 data by modifying *corrtag* files from LP3 programs 13931, "Third COS FUV Lifetime Position: Wavelength and Resolution Calibration (LCAL2)" (PI J. Roman-Duval), and 13932, "Third COS FUV Lifetime Position: Cross-Dispersion Profiles, Flux, and Flat-Field Calibration (LCAL3)" (PI J. Debes) based on the difference in modal gain between the LP3 and LP4 WCA regions. By applying the difference in modal gain to WCA data taken at LP3, we can change how the counts are flagged by CalCOS, which results in a general reduction in counts as well as creating gain-sag holes as would be seen at LP4.

For the WCA region at LP3, we used modal gain maps from program 12676, "COS/FUV Characterization of Detector Effects" (PI D. Massa). While this program was taken prior to the move to LP2, it mapped the entire detector and no light landed on the LP3 WCA region while at LP2, so there was no change in gain from when the data were taken and the start of LP3 in that region. This map was taken at high voltage (HV) levels of 169 and 167 for FUVA and FUVB respectively.

For the gain map at LP4, we used data obtained in program 14525, "Characterization of COS/FUV Detector Modal Gain at Lifetime Position 4" (PI D. Sahnow), which was executed during operations at LP3 and is the current state of the detector for the start of LP4 when the WCA falls on top of LP2. This program was taken at three HV values, 159/163/167 on FUVB and 163/167/171 on FUVA, respectively.

We scaled the LP3 gain map to match the LP4 HV levels by assuming 0.393 pulse height amplitude (PHA) bins per HV step. The two WCA regions are separated by the LP3-LP4 distance, or 32 pixels, so the LP4 WCA gain map region was shifted up to the same position as the LP3 WCA region, and then the scaled LP3 map was subtracted from the shifted LP4 map to create a delta-gain map. The new, simulated PHA values are calculated by adding the difference in gain to the original PHA values in the LP3 corrtags from programs 13931 and 13932 at the corresponding detector (XCORR, YCORR) locations.

### *2.2 Manually Modifying DQ Flags*

In addition to calculating PHA values, we also modified the data quality (DQ) flags in the *corrtag* files to ensure that CalCOS excluded the appropriate events that would correspond to a gain-sag hole or a lower-gain region. We set the PHA out-of-bounds flag (DQ = 512) for those events where the PHA was either less than 2 or greater than 23, and we set the gain-sag hole flag (DQ = 8192) for those events that fell in the region where the LP4 modal gain was less than 3 and within the active area of the detector.

### *2.3 Generating the Simulated LP4 Data*

We created several sets of the modified *corrtag* files with a range of shifts applied to the XCORR columns between $\pm$ 100 pixels in steps of 25 pixels. These sets simulate the OSM uncertainty resulting in a range of detector locations for lamp lines. The choice of sampling in the dispersion direction ensures that, within the simulated sets, some strong lines will fall inside and outside gain-sag holes. We then ran the modified *corrtag* files through CalCOS to produce simulated LP4 calibrated products.

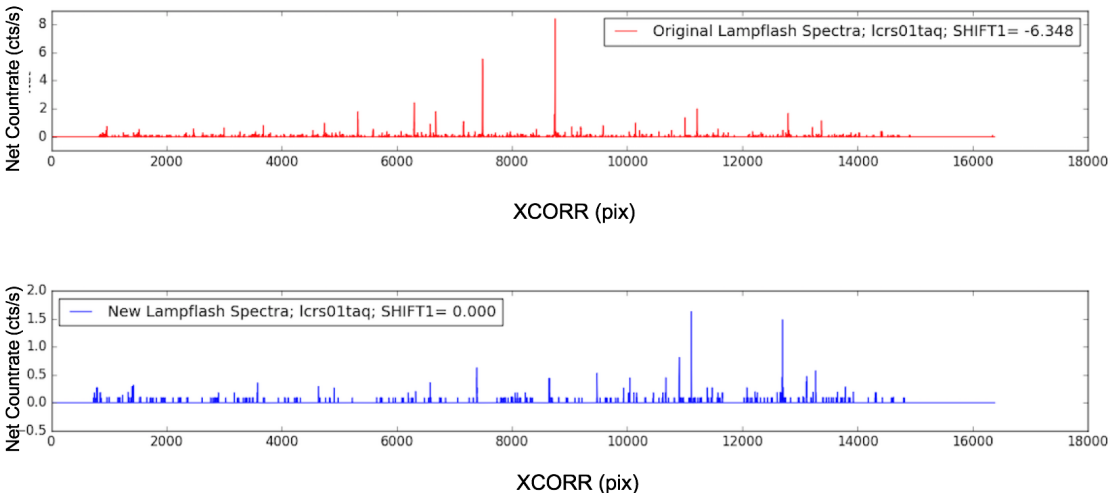


**Figure 1.** Example of a FUVB failed simulation: lcrs01taq. Net count rates are plotted as a function of XCORR pixel location on the detector. (These data are taken from the *lampflash* files produced by CalCOS.) The top panel is the original WCA spectrum, and the bottom panel is the simulated LP4 spectrum. Note that in the bottom spectrum, the two strongest lines between XCORR = 7000 and 9000 have been reduced to $\sim$ 0 counts $s^{-1}$, which results in CalCOS being unable to find the correct shift and returning a shift of 0.0 (after adjusting for the FP-POS).

**Table 1**. LP4 Simulations Derived from Program 13931 Where CalCOS Failed to Find a Shift

| Rootname | Grating | Cenwave | FP-POS | HV | Simulated OSM Uncertainty (pixels) |
|---|---|---|---|---|---|
| lcrs01t4q | G160M | 1623 | 1 | 163 | −50 |
| lcrs01taq | G160M | 1623 | 4 | 163 | −100 |
| lcrs51enq | G160M | 1623 | 1 | 163 | −25 |
| lcrs51enq | G160M | 1623 | 1 | 163 | −50 |
| lcrs51etq | G160M | 1623 | 4 | 163 | −100 |

**Table 2**. LP4 Simulations Derived from Program 13932 Where CalCOS Failed to Find a Shift

| Rootname | Grating | Cenwave | FP-POS | HV | Simulated OSM Uncertainty (pixels) |
|---|---|---|---|---|---|
| lcpb04j3s | G160M | 1623 | 3 | 163 | 100 |
| lcpb04j5s | G160M | 1623 | 4 | 163 | −75 |
| lcpb04j5s | G160M | 1623 | 4 | 163 | −100 |
| lcpb04j7s | G160M | 1611 | 1 | 163 | −25 |
| lcpb04j7s | G160M | 1611 | 1 | 163 | −50 |
| lcpb04j7s | G160M | 1611 | 1 | 163 | −75 |
| lcpb04j7s | G160M | 1611 | 1 | 163 | −100 |
| lcpb04j9s | G160M | 1611 | 2 | 163 | −50 |
| lcpb04j9s | G160M | 1611 | 2 | 163 | −75 |

### *2.4 WAVECORR Failures with Simulated Data*

WAVECORR failed to find a shift for the simulated G160M settings as strong lines shifted in and out of the simulated gain-sagged regions (Figure 1).

We give a summary of the LP4 simulations where CalCOS failed to find a shift in Tables 1 and 2. At HV = 163, there were only two settings where CalCOS failed to find a shift: G160M/1623 and G160M/1611 on segment FUVB. This is due to the strongest lines in the lamp spectra for these settings often both falling into a gain sag hole at the same time. From these results, we decided to create a program, 14869, for testing WAVECORR at LP4 with G160M/1623 and G160M/1611 observations.

## 3. Testing WAVECORR at LP4 with Observed WCA Spectra

### *3.1 Observing Strategy*

COS program 14869 was specifically designed to test the reliability and accuracy of the WAVECORR calibration step in CalCOS for settings G160M/1623 and G160M/1611. (These are the two settings where the wavecal spectra are most affected by the gain-sagged region at LP2.)

Program 14869 is divided into eight visits: one visit for each of the four FP-POS positions for both G160M/1611 (A1–A4 in the dataset name) and G160M/1623 (B1–B4 in the dataset name) settings. Each visit is comprised of one orbit in which there are 13 internal wavecal exposures. Of the 13 exposures, eight are taken at different along-dispersion (AD) positions at the LP4 cross-dispersion (XD) position, two references are taken at the nominal LP3 and LP4 positions (in AD and XD) at nominal HV (167/175 for segments FUVA and FUVB at LP3 respectively and 162/162 for LP4), and two additional exposures are taken at LP4 with higher HV (exposures 11 and 12 in Table 3). Each exposure in each visit is executed in the sequence shown in Table 3.

The AD aperture positions were chosen in steps of 18 aperture steps within $\pm$ 1/2 FP-POS in order to sample the gain-sagged region while simultaneously simulating the maximum offsets due to OSM uncertainty, which can be as large as $\pm$ 1/2 FP-POS. We use two LP3 and LP4 reference exposures taken at APERXPOS = 22 at the beginning and end of each visit to estimate OSM drift over the course of the orbit as described below. APERXPOS, which is found in the primary header of each data product, defines the position of the aperture in the AD direction and is equivalent to the telemetry keyword LAPDSTP. The LP3 references will also serve as zero-points for comparisons with the LP4 exposures. Two additional exposures at LP4 with APERXPOS = 22 were taken with raised HV levels of 165/165 (for segments A and B) and 167/167 for exposures 11 and 12 respectively. The additional exposures with raised HV are used as an additional test of the sensitivity of WAVECORR to the modal gain.

**Table 3**. Program 14869 Settings for Each Visit Sequence

| Exposure | PSA XD Position | Aperture Steps (APERXPOS) | FUVA/FUVB HV |
|---|---|---|---|
| 1 | LP3 | 22 | 167/175 |
| 2 | LP4 | 22 | 162/162 |
| 3 | LP4 | −32 | 162/162 |
| 4 | LP4 | −68 | 162/162 |
| 5 | LP4 | −50 | 162/162 |
| 6 | LP4 | 58 | 162/162 |
| 7 | LP4 | −14 | 162/162 |
| 8 | LP4 | −4 | 162/162 |
| 9 | LP4 | 40 | 162/162 |
| 10 | LP4 | 22 | 162/162 |
| 11 | LP4 | 22 | 165/165 |
| 12 | LP4 | 22 | 167/167 |
| 13 | LP3 | 22 | 167/175 |

Note. — APERXPOS of 22 is the zero-point or "home position" for the PSA.

**Table 4**. Calibration Settings for 14869 Pipeline Processing

| Calibration Step | Setting |
|---|---|
| FLATCORR | PERFORM |
| DEADCORR | PERFORM |
| DQICORR | PERFORM |
| TEMPCORR | PERFORM |
| GEOCORR | PERFORM |
| IGEOCORR | PERFORM |
| RANDCORR | PERFORM |
| WALKCORR | PERFORM |
| PHACORR | PERFORM |
| TRCECORR | OMIT |
| ALGNCORR | OMIT |
| XTRCTALG | BOXCAR |
| BADTCORR | OMIT |
| DOPPCORR | OMIT |
| HELCORR | OMIT |
| X1DCORR | PERFORM |
| BACKCORR | PERFORM |
| WAVECORR | PERFORM |
| FLUXCORR | OMIT |
| BRSTCORR | OMIT |
| TDSCORR | OMIT |

### *3.2 Initial Processing through CalCOS*

We used preliminary LP4 versions of the XTRACTAB, DISPTAB, and FLUXTAB calibration files for the extraction and WAVECORR calibration steps of the LP4 data obtained in program 14869. We also set the calibration switches according to Table 4. The results of the initial calibration show that only one exposure from program 14869, ldd9a3h4q, resulted in an incorrect WAVECORR result: the same WAVECORR failure to find a shift as seen in the simulated observations results in Section 2 (see Table 6).

### *3.3 Estimating and Removing OSM Drift*

We designed each visit such that the OSM would not be commanded to move for the duration of the visit and so that each exposure could be referenced to the initial exposure of the visit, thereby allowing us to estimate and remove OSM drift from further

**Table 5**. OSM Drift Rates for Each Segment and Visit in $10^{-4}$ pixels $s^{-1}$

| Visit | FUVA Drift Rate | FUVB Drift Rate |
|---|---|---|
| A1 | −4.48 | −4.88 |
| A2 | −1.21 | −2.21 |
| A3 | −1.06 | −1.08 |
| A4 | −5.31 | −4.55 |
| B1 | −6.03 | −4.85 |
| B2 | −6.98 | −6.19 |
| B3 | −5.32 | −5.05 |
| B4 | −9.34 | −7.94 |

calculations. Each visit was structured such that a reference exposure (nominal AD position, nominal HV) occurred at LP3 and LP4 at the beginning and end of the visit (LP3: exposures 1 and 13, LP4: exposures 2 and 10 from Table 3). Since the shift returned from CalCOS *should* be equal to the difference between the various AD positions in the sequence and the AD position of the *first* exposure in pixels, any remaining residual must therefore be due to OSM drift, error in the aperture-step-to-pixel conversion factor, and walk. To estimate the contribution from OSM drift, we assume that the drift rate is constant over the course of each visit and that negligible drift occurs during the course of each 48 s exposure. We compute the drift rate using the difference in shifts reported by CalCOS for the reference exposures and the time between those exposures. Using this approach, we then estimated and removed the drift that occurred in each exposure by multiplying the drift rates (shown by visit in Table 5) by the time elapsed since the start of the first exposure in the sequence and then subtracting that estimate from the SHIFT1 values. We provide an example of this measurement in Figure 2.

The total estimated drift for each visit is $\sim 2$ pixels or less as measured from the LP3 reference exposures (exposures 1 and 13 from Table 3). We chose not to use the LP4 references (exposures 2 and 10) due to the unknown effects of gain sag on the measured shift.

### *3.4 APERXPOS to Pixel Conversion*

Because offsets in the AD direction are commanded in units of aperture steps, it is necessary to know the step-to-pixel conversion to determine how far in pixels each wavecal spectrum is shifted from the reference position. The Phase II description of program 14869 gives the approximate conversion between aperture steps and pixels in the dispersion direction as $\approx$ 18 steps / 30 pixels. This comes from the plate scale of $0.0285''$ $pixel^{-1}$ reported in Table 1.1 of the COS Instrument Handbook (Fox et al.

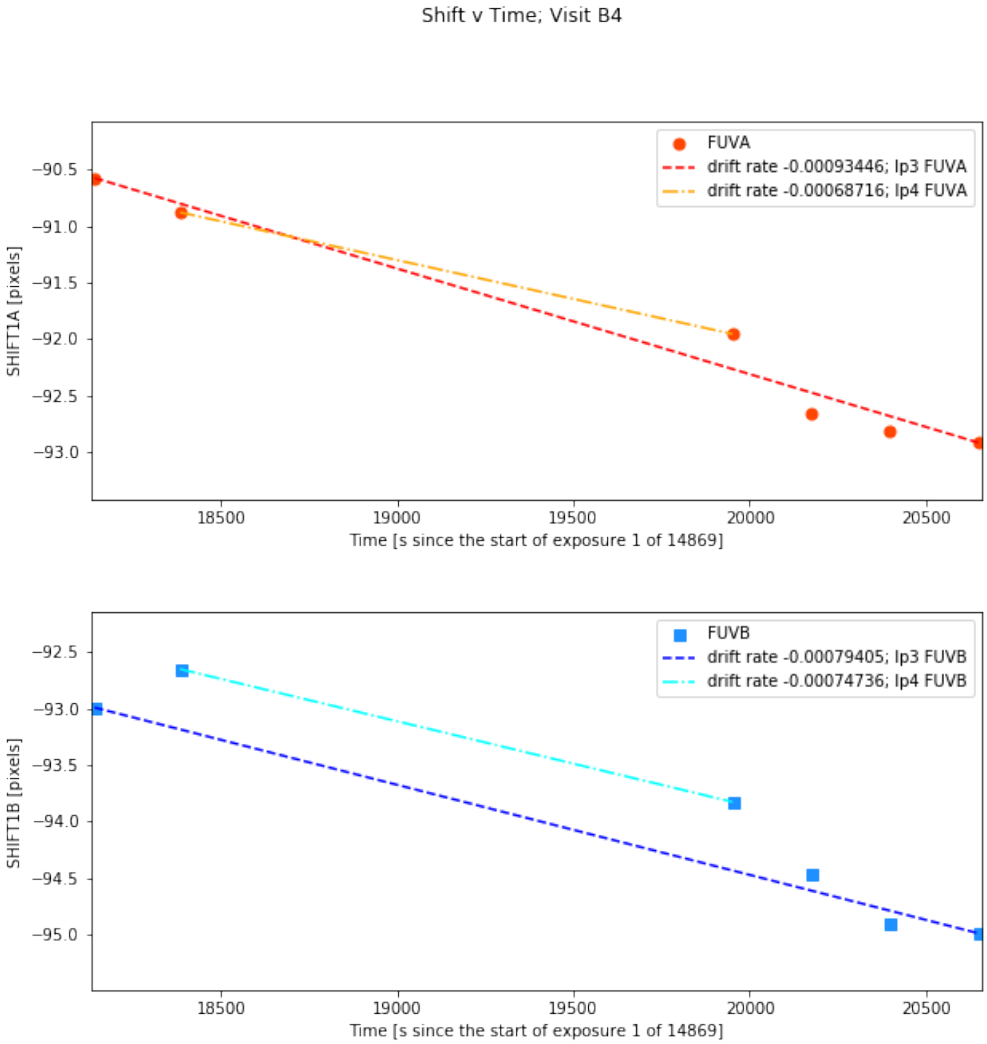


**Figure 2.** Example of OSM shifts over the course of visit B4 in program 14869. The top panel shows FUVA; the bottom panel shows FUVB. The drift rates in this figure are in units of pixels $s^{-1}$. From left to right, the data points correspond to exposures 1, 2, 10, 11, 12, and 13 from the visit structure outlined in Table 3. Note that exposures 11 and 12 were not used in measuring the linear drift.

2017), and the nominal relation of 21 steps / arcsecond, resulting in 0.5985 steps / pixel (1.67 pixels / step). However, the exact plate scale is dependent on grating and lifetime position, so this conversion factor may not apply to the observations in program 14869.

As part of our investigation, we independently measured the conversion factor between aperture steps and pixels by finding the slope of the best-fit line of the OSM drift-removed shift found by WAVECORR in pixels (SHIFT1) versus AD aperture position in units of aperture steps (APERXPOS) for segments A and B independently for each visit (Method 1). As verification, we also computed the conversion factor (defined

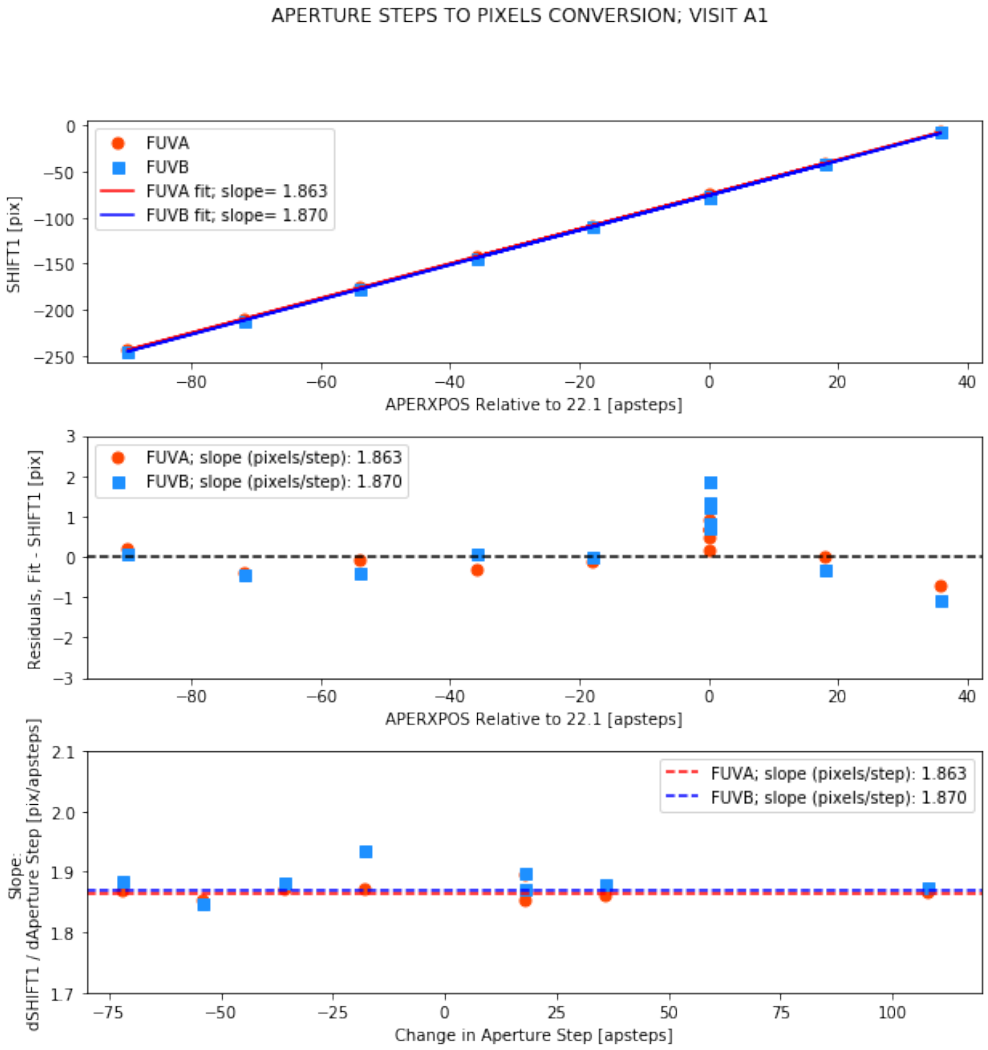


**Figure 3.** Example of measuring the conversion factor of 1.87 pixels / step for visit A1. *Top panel*: Method 1: Conversion factor measured by fitting a line to all SHIFT1 values in a visit (FUVA in red, FUVB in blue). *Middle*: Residuals between the line of best fit and the data points as a function of APERXPOS. *Bottom panel*: Method 2: Conversion factor measured using chronologically adjacent exposures; i.e., slopes measured between adjacent points (conversion factors plotted as red and blue points as a function of change in APERXPOS). Slopes from method 1 (top panel) are plotted as horizontal lines for FUVA (red dashed line) and FUVB (blue dashed line). The top two panels are relative to APERXPOS = 22.

in the same way as in Method 1: change in SHIFT1 over change in APERXPOS) between chronologically adjacent pairs in each visit (Method 2). Both methods can be seen in Figure 3.

Both methods agree well, with the largest residuals in Figure 3 coming from the

LP3 and high HV LP4 likely due to differences in the amount of walk. We measure the average conversion factor for both segments across all visits as $\approx 1.87$ pixels / step (1.866 pixels / step for FUVA and 1.865 pixels / step for FUVB) or $\approx 18$ steps / 33.7 pixels, which is a difference of about 11% in comparison to the conversion factor derived from the plate scale given in the COS Instrument Handbook.

### *3.5 WAVECORR Performance at LP4*

For each exposure, we run two tests to verify the results returned by the WAVECORR step of CalCOS. First, we measure the shift between the wavecal spectrum and its corresponding template in the LAMPTAB reference file by cross-correlating the two spectra. Second, we compute the residuals between the shift returned by CalCOS and the expected shift. For each exposure, the expected shift is a combination of OSM drift, FP-POS offset, and the commanded APERXPOS offset relative to the reference exposure in each visit.

Any remaining residuals are primarily the result of walk in the dispersion direction (X walk) and CalCOS computational error in determining the shift (see Section 4), which are the sources of error in WAVECORR that are potentially affected by changes in gain. X walk can affect CalCOS's ability to accurately calculate the location of spectral lines by decreasing the resolution of those lines due to individual events being mislocated, which cumulatively can result in lines being smeared in the dispersion direction. X walk can also result in entire spectral lines being shifted without affecting their resolution. This in turn increases the uncertainty of the cross-correlation in the WAVECORR routine via additional changes in the shape of the wavecal spectrum relative to the template spectrum.

The results of this analysis indicate that WAVECORR performed successfully and within expectations with the exception of the failed exposure, ldd9a3h4q. The results of the independent cross-correlation for each exposure can be seen in Tables 6 and 7 (found in the Appendix) with the failed exposure's rootname highlighted in red. As shown in Figure 4, residuals between the original WAVECORR results and the manual cross-correlation measurements are within the typical errors of CalCOS, which can be found in the *trl* files. On average, the residuals are less than a pixel for both FUVA and FUVB, with FUVB performing better due to the larger number of strong lines in the wavecal spectra for G160M/1611 and 1623, which offers a more robust cross-correlation.

The remaining offsets relative to the reference exposures (Tables 6 and 7) are between $-0.5$ and 3.5 pixels with the average offset being $\approx 0.67$ and $\approx 1.3$ pixels for FUVA and FUVB respectively (summarized in Figure 5). These results indicate that WAVECORR at LP4 will typically perform within expected errors of $\approx 3$ pixels or less.

For the one exposure where CalCOS failed to find a shift (ldd9a3h4q), the independent cross-correlation did not have the same problem. Understanding why CalCOS failed to find a shift for this exposure and the simulated exposures requires an understanding of how CalCOS calculates shifts and determines whether or not they are valid.

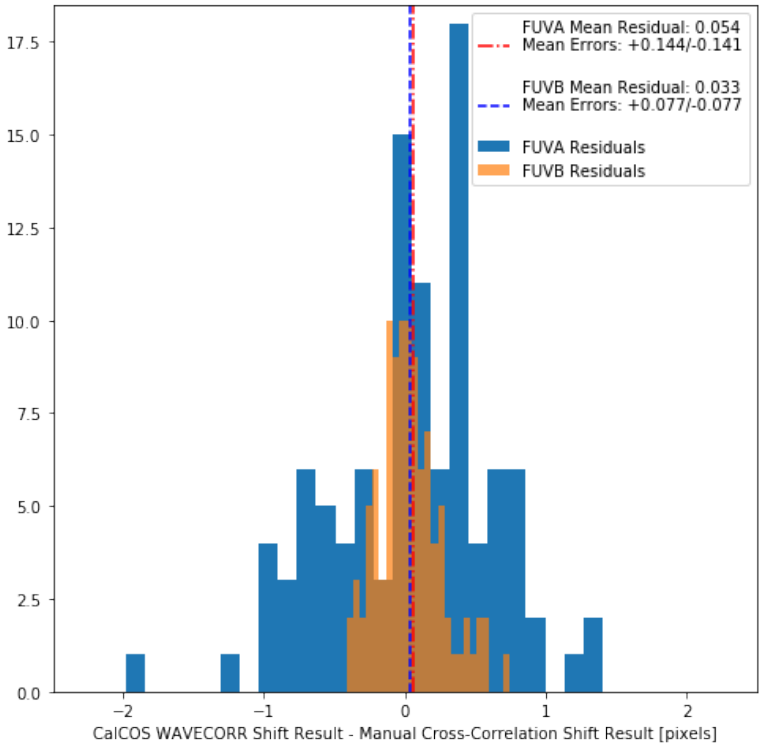


**Figure 4.** Histogram of the residuals between WAVECORR results and our manual measurements. The mean residuals denote the mean of the distribution of the residuals, and the mean errors denote the standard deviation of the distribution of the residuals. The failed exposure ldd9a3h4q is not included in this figure.

## 4. Shift Not Found by CalCOS

Of the 208 wavecal spectra taken during program 14869 (104 exposures with both FUVA and FUVB segments), only one was returned with a "shift not found" warning by CalCOS. Inspection of the spectrum extracted from the FUVB segment of exposure ldd9a3h4q (see Figure 6) shows that the two strongest emission lines are essentially missing as they fell in gain-sag holes. Using an internal-only version of CalCOS that returns specific reasons for why a shift is not found, we determined that the minimum reduced chi-squared value ($\chi^2_\nu$) was larger than a threshold value ($N_\sigma$) designed to reject poor matches between the WCA and template spectra. In CalCOS version 3.1.8 and earlier, $N_\sigma = 15$, and for exposure ldd9a3h4q, $\chi^2_\nu \approx 24$.

All of the exposures in this program had the Pt-Ne lamp turned on for 48 s. During standard science observations, the duration for which the Pt-Ne lamp is on is much shorter, only 12 s in general. Since the data were taken in TIME-TAG mode, we created 12 s versions of the exposures by selecting 12 s subsets of the data in order to investigate whether or not having fewer counts in the WCA spectrum affects the ability of CalCOS to determine shift values for wavelength calibration. When 48 s exposures were used,

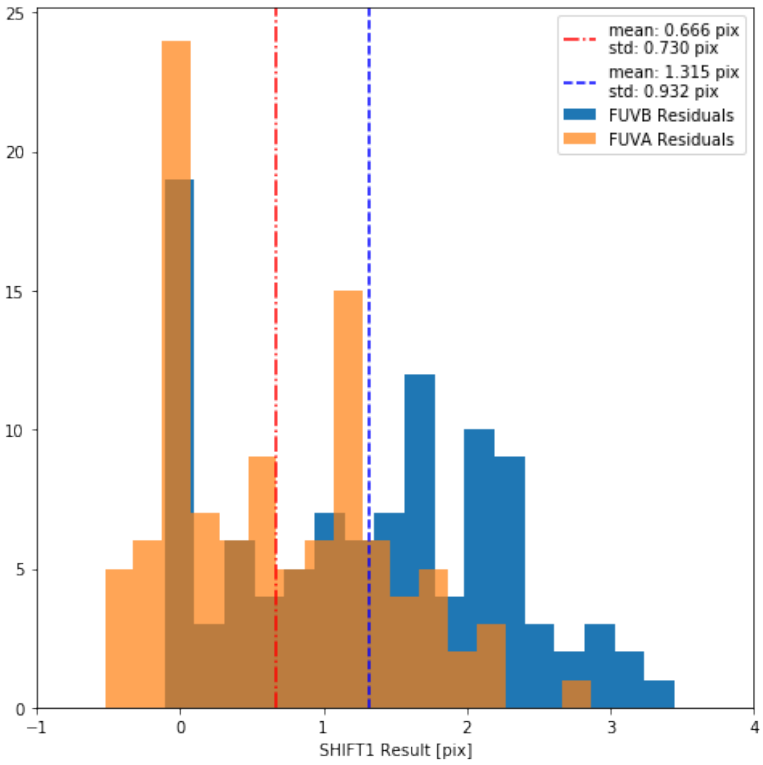


**Figure 5.** Histogram of WAVECORR shifts relative to the reference exposure (the first exposure) after OSM drift and the APERXPOS offset in pixels have been removed in each visit. The failed exposure ldd9a3h4q is not included.

there was only one exposure affected by a failure to find the shift in the WAVECORR step of CalCOS. In the 12 s dataset, there are five total spectra on FUVB where CalCOS fails to find a shift: ldd9a2e3q, ldd9a2eeq, ldd9a2egq, ldd9a3gpq, and ldd9a3h4q (again, as expected since ldd9a3h4q failed in the 48 s dataset). In the four new failures (ldd9a2e3q, ldd9a2eeq, ldd9a2egq, and ldd9a3gpq), the strongest Pt-Ne emission line is missing due to falling in a gain-sag hole. All five failures occur for the same reason as before, $\chi^2_\nu > N_\sigma$. However, as shown in Figure 7, where CalCOS is able to determine a shift, the exposure time does not seem to have any additional impact on the calculation.

### *4.1 How Does CalCOS Determine Shifts?*

All of the code that determines the shift in pixels between the template Pt-Ne spectrum and the wavecal spectrum is contained within the `findshift1.py` file that is part of the CalCOS library. The shift is determined as follows. The Pt-Ne template spectrum and observed WCA spectrum, referred to below as the arrays $tmpl$ and $spec$, respectively, are read in. The $XC\_range$ parameter in the WCPTAB is taken to be the maximum possible shift between the template and wavecal spectrum (i.e., the cross-

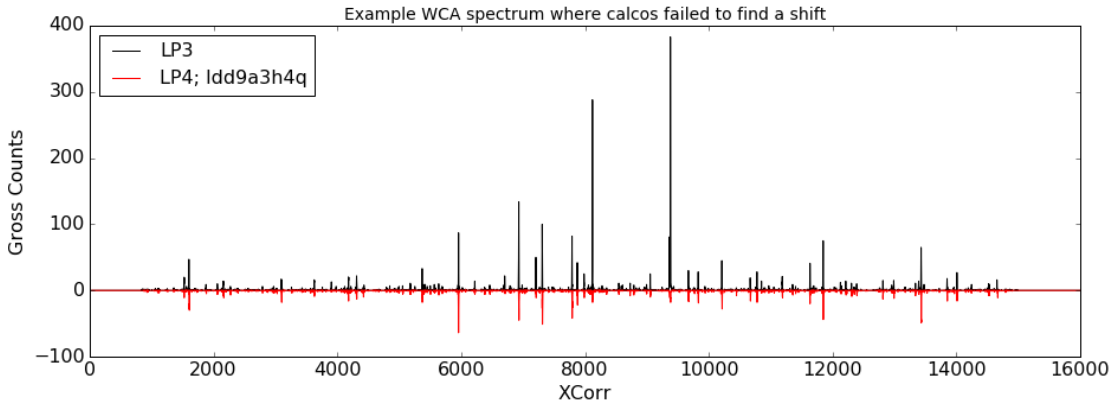


**Figure 6.** Example showing one spectrum where CalCOS failed to find a shift for the FUVB segment. The black spectrum is from an observation taken at LP3 and is shown here as a reference. The red spectrum, inverted for clarity, was taken at LP4 and is the lone spectrum for program 14869 for which CalCOS returned the error "shift not found." It is quite clear that the two strongest Pt-Ne emission lines are missing from the LP4 WCA spectrum, as they have fallen on severely gain-sagged regions of the detector. The simulated spectra had this same issue, as seen in Figure 1.

correlation routine checks shifts from $-XC\_range$ to $+XC\_range$). For each possible integer from $-XC\_range$ to $+XC\_range$, the following analysis is performed by the function `findShift`.

First, in the `computeNormalization` function the WCA spectrum is shifted with respect to the template spectrum by the integer value described above. Both spectra are then truncated to only include the overlap region (i.e., indices where both spectra contain data). If the edge of either spectrum contains a zero, both spectra are trimmed until neither end of both spectra is zero, leaving each spectrum with $n$ points. A scaling factor is computed as

$$factor = \frac{[\sum_i spec(i)][\sum_i tmpl(i)] - n \times \sum_i [tmpl(i) \times spec(i)]}{[\sum_i tmpl(i)][\sum_i tmpl(i)] - n \times \sum_i [tmpl(i) \times tmpl(i)]}, \quad (1)$$

where $spec(i)$ and $tmpl(i)$ are the number of counts in the spectra at "pixel" $i$. The denominator is always negative, and if $factor$ itself is negative then the calculation for that particular shift value is halted. If $factor$ is positive, the calculation continues. A parameter $baseline$ is calculated as

$$baseline = \frac{1}{n}\left(\sum_i spec(i) - factor \times \sum_i tmpl(i)\right), \quad (2)$$

and the purpose of these two variables is to scale the template spectrum to have roughly the same intensity as the WCA spectrum; i.e., $baseline + factor \times tmpl$ is roughly

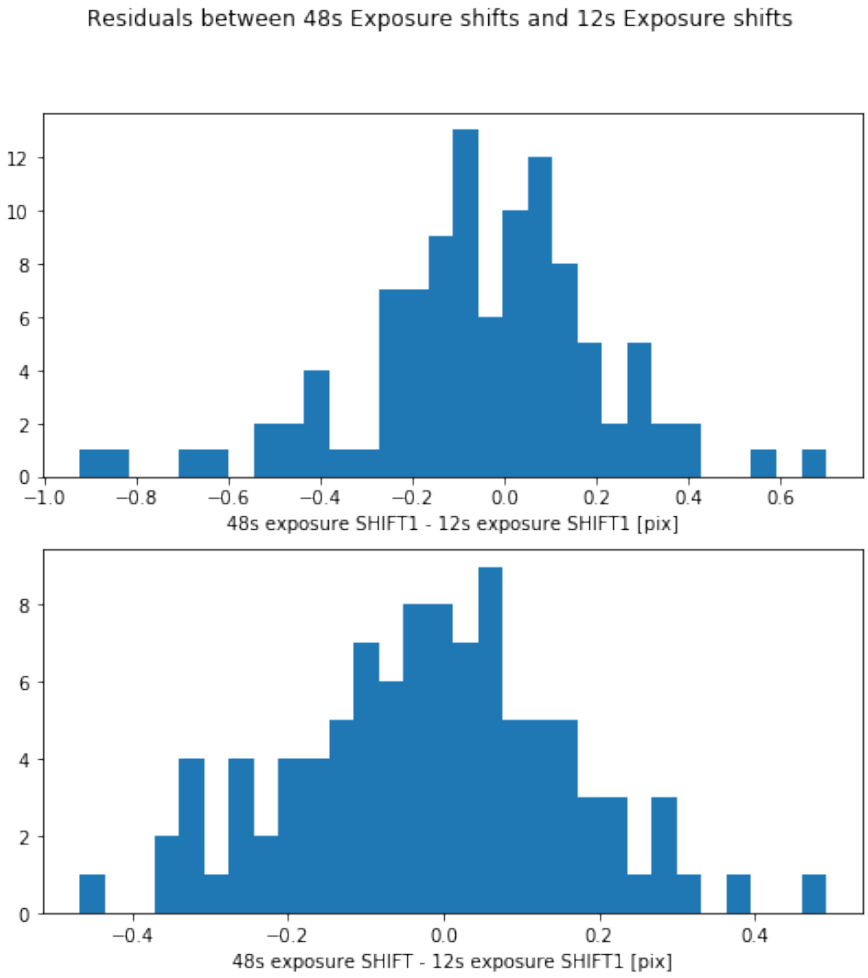


**Figure 7.** Distribution of the residuals between the SHIFT1 calculations returned by CalCOS between the 48 s data and the 12 s data for FUVA (top panel) and FUVB (bottom panel). Shifts where CalCOS gave the "shift not found" warning are not included. These residuals are within typical WAVECORR calculation error, and so the only difference between the 12 s data and the 48 s data is that the likelihood of CalCOS failing to find a shift is larger for the 12 s data.

normalized to match the observed WCA spectrum. The residuals between the WCA spectrum and scaled template spectrum are calculated as

$$residual = spec - (baseline + factor \times tmpl), \tag{3}$$

and the root-mean-squared (RMS) value of the residual spectrum is found:

$$\text{RMS} = \sqrt{\frac{\sum_i residual(i)^2}{n}}. \tag{4}$$

In this way, each potential shift from $-XC\_range$ to $+XC\_range$ with $factor > 0$ is assigned an RMS value.

Next, the calculation proceeds to the `computeChiSquare` function. Here, the spectrum is normalized to the template (reverse of above) as

$$spec_{norm} = \frac{(spec - baseline)}{factor}. \tag{5}$$

The uncertainty ($\sigma_i$) for each point in the difference between the template and normalized spectrum is found by adding the uncertainties of each in quadrature. Assuming Poisson statistics (valid given time-resolved photon counting) the uncertainty on the number of counts in each pixel in both $tmpl$ and $spec$ is approximated by the square root of the number of counts. The variance ($\sigma_i^2$) is then utilized in calculating the $\chi^2$ statistic

$$\chi^2 = \sum_i \frac{[spec_{norm}(i) - tmpl(i)]^2}{\sigma_i^2}, \tag{6}$$

and the number of degrees of freedom $\nu$ is taken to be the number of points where either the template or WCA spectrum is non-zero, minus 1. Both are returned by the `computeChiSquare` function.

Back within the `findShift` function the reduced $\chi^2$ values (i.e. $\chi^2_\nu = \chi^2/\nu$) are calculated for each potential shift value. The maximum value of $\chi^2_\nu$ calculated this way is assigned to all shifts for which the calculation was halted because the $factor$ parameter was negative. The routine then finds shift values where there are local minima in RMS, and checks the 10 smallest RMS local minima to determine which has the smallest $\chi^2_\nu$. A quadratic fit is performed on the $\chi^2_\nu$ curve from $k-2$ to $k+2$ (where $k$ is the index of the local minimum), and the location of the vertex of that quadratic is returned as the shift between the template and WCA spectra.

Beyond this analysis, there are other conditions which must be met for CalCOS to consider the calculation successful and return a shift. Two such conditions depend on the parameter $N_\sigma$, which is compared to the minimum $\chi^2_\nu$ which was used in finding the shift. If $\chi^2_\nu > N_\sigma$ or $\chi^2_\nu < 1/N_\sigma$ – corresponding to the classical cases of a model being a poor fit to the data and the model over-fitting the data, respectively – then the shift, even if found successfully, is rejected and set to zero. As mentioned previously, every time CalCOS failed to find a shift it was because $\chi^2_\nu > N_\sigma$.

If we relax this constraint by increasing $N_\sigma$ so that it is larger than the minimum $\chi^2_\nu$, CalCOS successfully finds the shift between the template and WCA spectra for *all* simulated and observed data (including the 12 s exposure time versions of program 14869).

We are confident that these shift values are correct for three reasons. First, $\chi^2_\nu$ as a function of shift shows a well-defined minimum, even if it is above the originally chosen cutoff of $N_\sigma = 15$. This is demonstrated in Figure 8. Second, the shifts determined for FUVA and FUVB agree with each other to within a few pixels, as expected. Finally, the shifts determined by CalCOS agree with those determined independently.

This, of course, raises the question: Why does CalCOS include $N_\sigma = 15$ as a cutoff for rejecting shift values? Standard practice when utilizing $\chi^2$ minimization is to

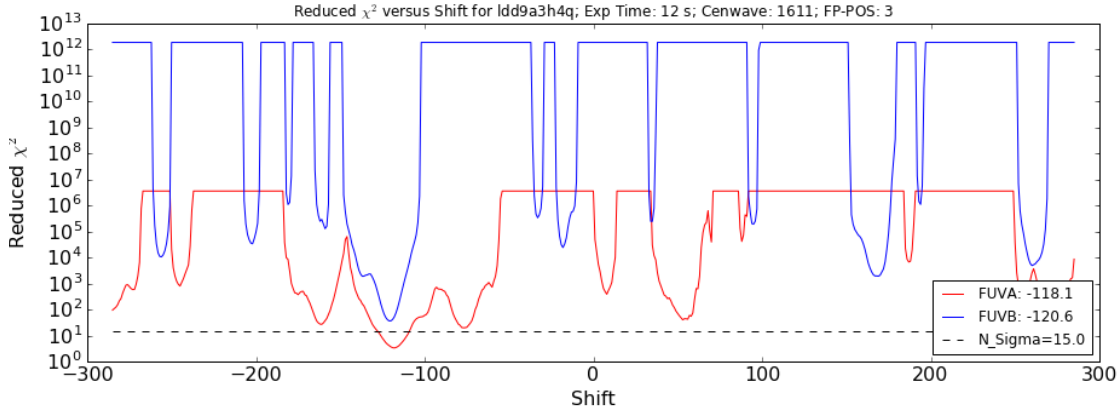


**Figure 8.** Reduced $\chi^2$ as a function of shift for the 12 s version of observation ldd9a3h4q on segments FUVA (red) and FUVB (blue). The horizontal dashed line marks $N_\sigma = 15$. CalCOS will fail to return a shift if $\chi^2_\nu$ does not pass below that line. In this example, the shift will successfully be found for FUVA, but *not* for FUVB.

reject models that result in $\chi^2_\nu \gg 1$ as poorly representing the data, and those that result in $\chi^2_\nu \ll 1$ as over-fitting the data (i.e., fitting noise features). In this case, however, we are not using a model but instead a template spectrum that is fixed. The template spectra were taken when the detector was "pristine," so all of the Pt-Ne emission lines are present and have the expected intensity ratios. Current wavecal spectra, however, may be missing lines that are present in the template because they fall in gain-sag holes, or they may have lines that differ in intensity ratio from the template because of gain-sag effects. As such, in some cases the template will *never* be a "good" model of the observed wavecal spectrum, meaning $\chi^2_\nu$ will be $\gg 1$ because possible discrepancies between select lines in the template and the observed spectrum raise the overall level of the $\chi^2_\nu$. Although the minimum $\chi^2_\nu$ value is large, it still represents the best match between the template and wavecal spectra.

### *4.2 Solution Applied*

Given our findings, it was decided that $N_\sigma$ would be increased for future observations at LP4. Rather than being hard-coded as a parameter in the file `findshift1.py`, it is now included in the WCPTAB reference file under the new "N_SIGMA" column and is currently set to 100 for each FUV setting as of this writing. This solution allows for flexibility for optimizing $N_\sigma$ thresholds for each grating. This change has been implemented in CalCOS version 3.2.1, released in April 2017.

## 5. Summary

Simulations and observations showed that the WAVECORR step of CalCOS at LP4 had a risk of failing to return the shift between the wavecal spectrum and template spectrum, which is required in the wavelength calibration process. This failure was caused by a $\chi^2_\nu$ statistic computed as part of the WAVECORR module exceeding the hardcoded $N_\sigma$ threshold (found in the `findshift1.py` routine). We find that upon raising this threshold, WAVECORR successfully finds the appropriate shift in agreement with independent measurements using a different method. We have implemented this fix by modifying CalCOS and the WCPTAB reference file to allow for the selection of a new $N_\sigma$ value of 100 depending on the lifetime position and grating.

Apart from the "shift not found" error, WAVECORR performs as expected with errors typically within $\pm$ 1.5 pixels as seen in Figure 5.

As part of this analysis, we recalculated the conversion between aperture steps in the along dispersion direction and pixels. We find a value of 1.87 pixels / aperture step, compared to 1.67 pixels / aperture step assumed during the Phase II preparation of program 14869. Differences are likely caused by the fact that the detector plate scale is dependent on grating and lifetime position.

## Change History for COS ISR 2018-15

Version 1: 4 February 2019 – Original Document

## References

Fox, A. J., et al. 2017, *Cosmic Origins Spectrograph Instrument Handbook*, Version 9.0 (Baltimore: STScI)

Keyes, C. D. 2011, Instrument Science Report COS 2011-04, "Details of COS TAG-FLASH Execution"

Sahnow, D. 2018, Technical Instrument Report COS 2018-03, "Using the FENA1 Data for Measuring Walk on the COS FUV Detector"

Sahnow, D. J., Oliveira, C., Aloisi, A., et al. 2011, Instrument Science Report COS 2011-05, "Gain Sag in the FUV Detector of the Cosmic Origins Spectrograph"

## Appendix

Tables 6 and 7 show the results of each step of this analysis for each exposure. These include the original SHIFT1 values calculated by CalCOS, OSM drift estimates, APERXPOS offsets in pixels (calculated from the measured conversion factor of 1.87 pixels / step) and remaining residuals after both the OSM drift and APERXPOS offsets are subtracted from the original SHIFT1 value. The failed exposure's rootname is highlighted in red.

**Table 6**. Analysis Results for G160M/1611

| Rootname | FP-POS | SHIFT1A | SHIFT1B | OSM Drift A | OSM Drift B | APERXPOS Offset A | APERXPOS Offset B | Final Residuals A | Final Residuals B |
|---|---|---|---|---|---|---|---|---|---|
| ldd9a1d5q | 1 | −76.03 | −78.48 | −0.00 | −0.00 | 0.00 | 0.00 | 0.00 | 0.00 |
| ldd9a1d7q | 1 | −75.93 | −77.47 | −0.11 | −0.12 | 0.00 | 0.00 | 0.21 | 1.13 |
| ldd9a1d9q | 1 | −176.09 | −177.39 | −0.20 | −0.21 | −100.77 | −100.72 | 0.92 | 2.02 |
| ldd9a1dbq | 1 | −243.55 | −245.26 | −0.28 | −0.31 | −167.96 | −167.87 | 0.73 | 1.40 |
| ldd9a1ddq | 1 | −209.50 | −211.21 | −0.37 | −0.41 | −134.37 | −134.30 | 1.28 | 1.97 |
| ldd9a1dfq | 1 | −8.00 | −8.76 | −0.46 | −0.50 | 67.18 | 67.15 | 1.31 | 3.07 |
| ldd9a1dhq | 1 | −142.67 | −144.59 | −0.55 | −0.60 | −67.18 | −67.15 | 1.09 | 1.63 |
| ldd9a1djq | 1 | −109.40 | −110.98 | −0.64 | −0.69 | −33.59 | −33.57 | 0.86 | 1.76 |
| ldd9a1dlq | 1 | −42.52 | −43.44 | −0.72 | −0.79 | 33.59 | 33.57 | 0.65 | 2.25 |
| ldd9a1dnq | 1 | −76.31 | −78.35 | −0.81 | −0.88 | 0.00 | 0.00 | 0.53 | 1.01 |
| ldd9a1dqq | 1 | −76.93 | −78.85 | −0.91 | −0.99 | 0.00 | 0.00 | 0.01 | 0.62 |
| ldd9a1dsq | 1 | −77.25 | −79.07 | −1.01 | −1.10 | 0.00 | 0.00 | −0.20 | 0.51 |
| ldd9a1duq | 1 | −77.16 | −79.70 | −1.12 | −1.22 | 0.00 | 0.00 | 0.00 | 0.00 |
| ldd9a2e0q | 2 | −88.38 | −90.89 | −0.00 | −0.00 | 0.00 | 0.00 | 0.00 | 0.00 |
| ldd9a2e3q | 2 | −88.30 | −88.64 | −0.03 | −0.05 | 0.00 | 0.00 | 0.11 | 2.30 |
| ldd9a2e5q | 2 | −188.52 | −189.40 | −0.05 | −0.10 | −100.77 | −100.72 | 0.68 | 2.32 |
| ldd9a2e7q | 2 | −256.86 | −257.37 | −0.08 | −0.14 | −167.96 | −167.87 | −0.44 | 1.53 |
| ldd9a2eaq | 2 | −222.37 | −223.38 | −0.14 | −0.26 | −134.37 | −134.30 | 0.52 | 2.06 |
| ldd9a2ecq | 2 | −20.11 | −22.51 | −0.17 | −0.30 | 67.18 | 67.15 | 1.25 | 1.54 |
| ldd9a2eeq | 2 | −155.69 | −156.42 | −0.19 | −0.35 | −67.18 | −67.15 | 0.07 | 1.97 |
| ldd9a2egq | 2 | −122.55 | −122.78 | −0.21 | −0.39 | −33.59 | −33.57 | −0.37 | 2.07 |
| ldd9a2eiq | 2 | −54.15 | −55.90 | −0.24 | −0.43 | 33.59 | 33.57 | 0.88 | 1.85 |
| ldd9a2ekq | 2 | −89.11 | −89.52 | −0.26 | −0.48 | 0.00 | 0.00 | −0.47 | 1.85 |
| ldd9a2emq | 2 | −89.19 | −90.08 | −0.29 | −0.53 | 0.00 | 0.00 | −0.52 | 1.33 |
| ldd9a2eoq | 2 | −89.17 | −90.45 | −0.31 | −0.57 | 0.00 | 0.00 | −0.47 | 1.01 |
| ldd9a2eqq | 2 | −88.73 | −91.52 | −0.34 | −0.63 | 0.00 | 0.00 | 0.00 | 0.00 |
| ldd9a3gnq | 3 | −85.94 | −88.98 | −0.00 | −0.00 | 0.00 | 0.00 | 0.00 | 0.00 |
| ldd9a3gpq | 3 | −84.72 | −86.83 | −0.03 | −0.03 | 0.00 | 0.00 | 1.25 | 2.17 |
| ldd9a3grq | 3 | −184.61 | −187.58 | −0.05 | −0.05 | −100.77 | −100.72 | 2.15 | 2.17 |
| ldd9a3guq | 3 | −252.79 | −255.49 | −0.07 | −0.07 | −167.96 | −167.87 | 1.18 | 1.44 |
| ldd9a3gwq | 3 | −218.22 | −220.51 | −0.09 | −0.09 | −134.37 | −134.30 | 2.17 | 2.86 |
| ldd9a3gyq | 3 | −16.00 | −19.27 | −0.11 | −0.11 | 67.18 | 67.15 | 2.86 | 2.68 |
| ldd9a3h0q | 3 | −151.60 | −153.77 | −0.13 | −0.13 | −67.18 | −67.15 | 1.65 | 2.50 |
| ldd9a3h4q | 3 | −118.20 | 0.00 | −0.15 | −0.15 | −33.59 | −33.57 | 1.48 | 122.71 |
| ldd9a3h6q | 3 | −50.53 | −53.02 | −0.21 | −0.21 | 33.59 | 33.57 | 2.03 | 2.60 |
| ldd9a3h8q | 3 | −85.15 | −87.11 | −0.23 | −0.23 | 0.00 | 0.00 | 1.02 | 2.10 |

**Table 6.** (cont'd)

| Rootname | FP-POS | SHIFT1A | SHIFT1B | OSM Drift A | OSM Drift B | APERXPOS Offset A | APERXPOS Offset B | Final Residuals A | Final Residuals B |
|---|---|---|---|---|---|---|---|---|---|
| ldd9a3haq | 3 | −85.72 | −88.18 | −0.25 | −0.26 | 0.00 | 0.00 | 0.47 | 1.05 |
| ldd9a3hcq | 3 | −85.94 | −88.22 | −0.28 | −0.28 | 0.00 | 0.00 | 0.28 | 1.04 |
| ldd9a3heq | 3 | −86.24 | −89.29 | −0.30 | −0.31 | 0.00 | 0.00 | 0.00 | 0.00 |
| ldd9a4hsq | 4 | −76.19 | −80.78 | −0.00 | −0.00 | 0.00 | 0.00 | 0.00 | 0.00 |
| ldd9a4huq | 4 | −75.75 | −79.21 | −0.13 | −0.11 | 0.00 | 0.00 | 0.57 | 1.68 |
| ldd9a4hwq | 4 | −175.46 | −179.94 | −0.23 | −0.20 | −100.77 | −100.72 | 1.74 | 1.76 |
| ldd9a4i0q | 4 | −243.37 | −247.50 | −0.34 | −0.29 | −167.96 | −167.87 | 1.11 | 1.44 |
| ldd9a4i2q | 4 | −209.34 | −213.23 | −0.44 | −0.38 | −134.37 | −134.30 | 1.66 | 2.23 |
| ldd9a4i4q | 4 | −7.88 | −10.65 | −0.55 | −0.47 | 67.18 | 67.15 | 1.67 | 3.45 |
| ldd9a4i7q | 4 | −143.16 | −146.96 | −0.83 | −0.71 | −67.18 | −67.15 | 1.05 | 1.68 |
| ldd9a4i9q | 4 | −110.02 | −113.85 | −0.94 | −0.80 | −33.59 | −33.57 | 0.70 | 1.31 |
| ldd9a4ibq | 4 | −43.00 | −46.06 | −1.04 | −0.89 | 33.59 | 33.57 | 0.65 | 2.04 |
| ldd9a4idq | 4 | −77.31 | −80.82 | −1.15 | −0.98 | 0.00 | 0.00 | 0.03 | 0.94 |
| ldd9a4ifq | 4 | −77.45 | −81.39 | −1.26 | −1.08 | 0.00 | 0.00 | 0.01 | 0.47 |
| ldd9a4ihq | 4 | −77.55 | −81.53 | −1.38 | −1.18 | 0.00 | 0.00 | 0.03 | 0.43 |
| ldd9a4ijq | 4 | −77.71 | −82.08 | −1.52 | −1.30 | 0.00 | 0.00 | 0.00 | 0.00 |

Note. — Each column is in pixels, and A/B denotes FUVA or FUVB. OSM Drift A and B columns are the estimated shifts. APERXPOS Offset A and B columns are the aperture offsets using the conversion factor of 1.87 pixels / step calculated as part of this analysis. Final Residuals A and B columns are calculated by subtracting the OSM drift and APERXPOS offset from the SHIFT1 values; they are relative to the reference exposure in each visit.

**Table 7**. Analysis Results for G160M/1623

| Rootname | FP-POS | SHIFT1A | SHIFT1B | OSM Drift A | OSM Drift B | APERXPOS Offset A | APERXPOS Offset B | Final Residuals A | Final Residuals B |
|---|---|---|---|---|---|---|---|---|---|
| ldd9b1inq | 1 | −86.28 | −89.17 | −0.00 | −0.00 | 0.00 | 0.00 | 0.00 | 0.00 |
| ldd9b1ipq | 1 | −86.10 | −87.54 | −0.15 | −0.12 | 0.00 | 0.00 | 0.33 | 1.74 |
| ldd9b1irq | 1 | −186.09 | −187.42 | −0.26 | −0.21 | −100.77 | −100.72 | 1.23 | 2.69 |
| ldd9b1itq | 1 | −254.21 | −255.64 | −0.38 | −0.31 | −167.96 | −167.87 | 0.42 | 1.71 |
| ldd9b1ivq | 1 | −219.15 | −220.80 | −0.50 | −0.40 | −134.37 | −134.30 | 2.00 | 3.07 |
| ldd9b1ixq | 1 | −18.27 | −19.64 | −0.62 | −0.50 | 67.18 | 67.15 | 1.45 | 2.88 |
| ldd9b1izq | 1 | −152.89 | −154.07 | −0.74 | −0.59 | −67.18 | −67.15 | 1.31 | 2.84 |
| ldd9b1j1q | 1 | −119.80 | −121.13 | −0.86 | −0.69 | −33.59 | −33.57 | 0.93 | 2.30 |
| ldd9b1j3q | 1 | −52.24 | −54.06 | −0.97 | −0.78 | 33.59 | 33.57 | 1.42 | 2.32 |
| ldd9b1j5q | 1 | −86.65 | −88.45 | −1.09 | −0.88 | 0.00 | 0.00 | 0.73 | 1.60 |
| ldd9b1j7q | 1 | −87.31 | −89.34 | −1.23 | −0.99 | 0.00 | 0.00 | 0.20 | 0.82 |
| ldd9b1j9q | 1 | −87.37 | −89.78 | −1.36 | −1.10 | 0.00 | 0.00 | 0.28 | 0.49 |
| ldd9b1jbq | 1 | −87.80 | −90.39 | −1.51 | −1.22 | 0.00 | 0.00 | 0.00 | 0.00 |
| ldd9b2jmq | 2 | −92.80 | −95.40 | −0.00 | −0.00 | 0.00 | 0.00 | 0.00 | 0.00 |
| ldd9b2joq | 2 | −92.40 | −94.28 | −0.17 | −0.15 | 0.00 | 0.00 | 0.56 | 1.27 |
| ldd9b2jqq | 2 | −192.50 | −194.10 | −0.31 | −0.27 | −100.77 | −100.72 | 1.38 | 2.30 |
| ldd9b2jsq | 2 | −260.67 | −262.34 | −0.44 | −0.39 | −167.96 | −167.87 | 0.53 | 1.33 |
| ldd9b2juq | 2 | −226.02 | −227.96 | −0.58 | −0.51 | −134.37 | −134.30 | 1.72 | 2.26 |
| ldd9b2jwq | 2 | −24.10 | −26.51 | −0.72 | −0.64 | 67.18 | 67.15 | 2.23 | 2.38 |
| ldd9b2jyq | 2 | −159.65 | −161.91 | −0.85 | −0.76 | −67.18 | −67.15 | 1.18 | 1.40 |
| ldd9b2k0q | 2 | −126.36 | −128.17 | −0.99 | −0.88 | −33.59 | −33.57 | 1.02 | 1.68 |
| ldd9b2k2q | 2 | −59.09 | −61.19 | −1.13 | −1.00 | 33.59 | 33.57 | 1.24 | 1.64 |
| ldd9b2k4q | 2 | −93.86 | −95.61 | −1.26 | −1.12 | 0.00 | 0.00 | 0.20 | 0.92 |
| ldd9b2k6q | 2 | −94.05 | −96.10 | −1.42 | −1.26 | 0.00 | 0.00 | 0.17 | 0.56 |
| ldd9b2k8q | 2 | −94.15 | −96.37 | −1.58 | −1.40 | 0.00 | 0.00 | 0.23 | 0.43 |
| ldd9b2kaq | 2 | −94.55 | −96.95 | −1.75 | −1.55 | 0.00 | 0.00 | 0.00 | 0.00 |
| ldd9b3kgq | 3 | −88.08 | −90.32 | −0.00 | −0.00 | 0.00 | 0.00 | 0.00 | 0.00 |
| ldd9b3kkq | 3 | −88.38 | −90.25 | −0.13 | −0.12 | 0.00 | 0.00 | −0.17 | 0.18 |
| ldd9b3kmq | 3 | −187.58 | −189.94 | −0.23 | −0.22 | −100.77 | −100.72 | 1.50 | 1.32 |
| ldd9b3kpq | 3 | −255.87 | −257.28 | −0.34 | −0.32 | −167.96 | −167.87 | 0.50 | 1.23 |
| ldd9b3krq | 3 | −221.66 | −223.27 | −0.44 | −0.42 | −134.37 | −134.30 | 1.22 | 1.76 |
| ldd9b3kvq | 3 | −20.22 | −22.02 | −0.55 | −0.52 | 67.18 | 67.15 | 1.22 | 1.67 |
| ldd9b3kxq | 3 | −154.78 | −156.98 | −0.65 | −0.62 | −67.18 | −67.15 | 1.13 | 1.10 |
| ldd9b3kzq | 3 | −122.12 | −123.68 | −0.75 | −0.72 | −33.59 | −33.57 | 0.30 | 0.92 |
| ldd9b3l2q | 3 | −54.97 | −56.90 | −1.04 | −0.99 | 33.59 | 33.57 | 0.56 | 0.83 |
| ldd9b3l4q | 3 | −89.21 | −91.29 | −1.15 | −1.09 | 0.00 | 0.00 | 0.01 | 0.12 |

**Table 7.** (cont'd)

| Rootname | FP-POS | SHIFT1A | SHIFT1B | OSM Drift A | OSM Drift B | APERXPOS Offset A | APERXPOS Offset B | Final Residuals A | Final Residuals B |
|---|---|---|---|---|---|---|---|---|---|
| ldd9b3l6q | 3 | −89.50 | −91.58 | −1.27 | −1.20 | 0.00 | 0.00 | −0.16 | −0.07 |
| ldd9b3l8q | 3 | −89.73 | −91.66 | −1.38 | −1.31 | 0.00 | 0.00 | −0.27 | −0.03 |
| ldd9b3laq | 3 | −89.59 | −91.76 | −1.52 | −1.44 | 0.00 | 0.00 | 0.00 | 0.00 |
| ldd9b4m9q | 4 | −90.57 | −92.99 | −0.00 | −0.00 | 0.00 | 0.00 | 0.00 | 0.00 |
| ldd9b4mbq | 4 | −90.88 | −92.65 | −0.23 | −0.19 | 0.00 | 0.00 | −0.08 | 0.53 |
| ldd9b4mdq | 4 | −190.63 | −192.59 | −0.41 | −0.35 | −100.77 | −100.72 | 1.13 | 1.47 |
| ldd9b4mfq | 4 | −259.10 | −261.02 | −0.59 | −0.50 | −167.96 | −167.87 | 0.02 | 0.35 |
| ldd9b4mkq | 4 | −224.00 | −225.95 | −0.78 | −0.66 | −134.37 | −134.30 | 1.72 | 2.00 |
| ldd9b4mmq | 4 | −22.62 | −24.62 | −0.96 | −0.81 | 67.18 | 67.15 | 1.73 | 2.04 |
| ldd9b4moq | 4 | −157.63 | −158.60 | −1.14 | −0.97 | −67.18 | −67.15 | 1.27 | 2.52 |
| ldd9b4mqq | 4 | −124.23 | −125.66 | −1.32 | −1.13 | −33.59 | −33.57 | 1.26 | 2.04 |
| ldd9b4mtq | 4 | −57.30 | −59.75 | −1.51 | −1.28 | 33.59 | 33.57 | 1.19 | 0.95 |
| ldd9b4mwq | 4 | −91.95 | −93.83 | −1.69 | −1.44 | 0.00 | 0.00 | 0.31 | 0.60 |
| ldd9b4mzq | 4 | −92.66 | −94.46 | −1.90 | −1.62 | 0.00 | 0.00 | −0.18 | 0.15 |
| ldd9b4n3q | 4 | −92.82 | −94.89 | −2.11 | −1.79 | 0.00 | 0.00 | −0.14 | −0.11 |
| ldd9b4n9q | 4 | −92.92 | −94.98 | −2.34 | −1.99 | 0.00 | 0.00 | 0.00 | 0.00 |

Note. — Same format as Table 6.